Stepanenko OV, Roginskii DO, Stepanenko OV, Kuznetsova IM, Uversky VN, Turoverov KK. 2016. Structure and stability of recombinant bovine odorant-binding protein: I. Design and analysis of monomeric mutants. PeerJ 4:e1933 https://doi.org/10.7717/peerj.1933

Structure and stability of recombinant bovine odorant-binding protein: I. Design and analysis of monomeric mutants

Olga V Stepanenko, Denis O Roginskii, Olesya V Stepanenko, Irina M Kuznetsova, Vladimir N Uversky, Konstantin K Turoverov

Bovine odorant-binding protein (bOBP) differs from other lipocalins by lacking the conserved disulfide bond and being able to form the domain-swapped dimers. To identify structural features responsible for the formation of the bOBP unique dimeric structure and to understand the role of the domain swapping on maintaining the native structure of the protein, structural properties of the recombinant wild type bOBP and its mutant that cannot dimerize via the domain swapping were analyzed. We also looked at the effect of the disulfide bond by designing a monomeric bOBPs with restored disulfide bond which is conserved in other lipocalins. Finally, to understand which features in the microenvironment of the bOBP tryptophan residues play a role in the defining peculiarities of the intrinsic fluorescence of this protein we designed and investigated single-tryptophan mutants of the monomeric bOBP. Our analysis revealed that the insertion of the glycine after the residue 121 of the bOBP prevents domain swapping and generates a stable monomeric protein bOBP-Gly121+. We also show that the restored disulfide bond in the GCC-bOBP mutant leads to the noticeable stabilization of the monomeric structure. Structural and functional analysis revealed that none of the amino acid substitutions introduced to the bOBP affected functional activity of the protein and that the ligand binding leads to the formation of a more compact and stable state of the recombinant bOBP and its mutant monomeric forms. Finally, analysis of the single-tryptophan mutants of the monomeric bOBP gave us a unique possibility to find peculiarities of the microenvironment of tryptophan residues which were not previously described.

PeerJ PrePrints | https://dx.doi.org/10.7287/peerj.preprints.1445v1 | CC-BY 4.0 Open Access | rec: 23 Oct 2015, publ: 23 Oct 2015

Structure and Stability of Recombinant Bovine Odorant-Binding Protein: I. Design and Analysis of Monomeric Mutants

Olga V. Stepanenko,[1] Denis O. Roginskii,[1] Olesya V. Stephanenko,[1] Irina M. Kuznetsova,[1] Vladimir N. Uversky,[1,2,*] and Konstantin K. Turoverov[1,3,*]

[1]*Laboratory of structural dynamics, stability and folding of proteins, Institute of Cytology, Russian Academy of Sciences, St. Petersburg, Russia;*

[2]*Department of Molecular Medicine and USF Health Byrd Alzheimer's Research Institute, Morsani College of Medicine, University of South Florida, Tampa, FL, USA;*

[3]*Peter the Great St. Petersburg Polytechnic University, St. Petersburg, Russia*

***To whom correspondence should be addressed**: VNU, Department of Molecular Medicine, University of South Florida, 12901 Bruce B. Downs Blvd. MDC07, Tampa, Florida 33612, USA, E-mail: vuversky@health.usf.edu; KKT, Institute of Cytology, Russian Academy of Sciences, Tikhoretsky Av., 4, St. Petersburg 194064, Russia, E-mail: kkt@incras.ru

Running title: Monomeric forms of bOBP

ABSTRACT

Bovine odorant-binding protein (bOBP) differs from other lipocalins by lacking the conserved disulfide bond and being able to form the domain-swapped dimers. To identify structural features responsible for the formation of the bOBP unique dimeric structure and to understand the role of the domain swapping on maintaining the native structure of the protein, structural properties of the recombinant wild type bOBP and its mutant that cannot dimerize via the domain swapping were analyzed. We also looked at the effect of the disulfide bond by designing a monomeric bOBPs with restored disulfide bond which is conserved in other lipocalins. Finally, to understand which features in the microenvironment of the bOBP tryptophan residues play a role in the defining peculiarities of the intrinsic fluorescence of this protein we designed and investigated single-tryptophan mutants of the monomeric bOBP. Our analysis revealed that the insertion of the glycine after the residue 121 of the bOBP prevents domain swapping and generates a stable monomeric protein bOBP-Gly121+. We also show that the restored disulfide bond in the GCC-bOBP mutant leads to the noticeable stabilization of the monomeric structure. Structural and functional analysis revealed that none of the amino acid substitutions introduced to the bOBP affected functional activity of the protein and that the ligand binding leads to the formation of a more compact and stable state of the recombinant bOBP and its mutant monomeric forms. Finally, analysis of the single-tryptophan mutants of the monomeric bOBP gave us a unique possibility to find peculiarities of the microenvironment of tryptophan residues which were not previously described.

Key words: odorant-binding protein; domain swapping; fluorescence; circular dichroism; protein; chemical denaturation

Abbreviations: bOBP, bovine odorant-binding protein; pOBP, porcine odorant-binding protein; GdnHCl, guanidine hydrochloride; CD, circular dichroism; UV, ultra-violet; Parameter *A*, (I_{320}/I_{365}) upon excitation at λ_{ex} = 297 nm.

INTRODUCTION

Lipocalins constitute a family of carrier proteins that transport various small hydrophobic molecules ranging from lipids to retinoids, steroids, and bilins. Being found in animals, plants, and bacteria and possessing low sequence identity (less than 20 %), these proteins are characterized by the presence of the conserved "lipocalin fold" that includes two structural modules, an eight-stranded β-barrel that constitutes 70-80% of the protein and includes the ligand-binding site and a C-terminal α-helix with unknown function (Flower et al. 2000). Evolution of the lipocalin fold generated numerous specialized carrier proteins with the highly diversified binding specificities.

One of the sub-classes of the lipocalin family includes odorant binding proteins (OBPs) with the characteristic ability of reversible binding of various odorant molecules; i.e. volatile, small and hydrophobic compounds with no fixed structure and chemical properties (Tegoni et al. 2000). Classic odorant binding protein (OBP) is characterized by a specific monomeric fold, where the eight β-strands, a short α-helical region, and the ninth β-strand interact to form a β-barrel followed by the disordered C-terminal tail (Bianchet et al. 1996; Flower et al. 2000). The ligand binding site of these proteins is formed by hydrophobic and aromatic residues located within the inner cavity of the β-barrel and loop regions connecting β-strands of the barrel. The conserved disulfide bridge formed by Cys 63 and Cys 155 is commonly found in many OBPs to link the flexible C-terminal moiety and strand β4.

Curiously, despite rather high sequence identity between porcine and bovine OBPs (42%), these lipocalins are characterized by different quaternary structures, with porcine OBP (pOBP) being a monomeric protein (Spinelli et al. 1998), and with bovine OBP (bOBP) being a dimer (Bianchet et al. 1996; Tegoni et al. 1996), protomers of which lack the disulfide bridge

which is a common feature for all lipocalin family members (Tegoni et al. 2000). Therefore, bOBP has a unique dimeric structure, which is quite different from the monomeric folds of the majority of classical OBPs (Bianchet et al. 1996; Stepanenko et al. 2014b) (Figure 1). In the bOBP dimer, each of the two protomers forms a β-barrel that interacts with the α-helical portion of the C-terminal tail of other protomer via the domain swapping mechanism. Such a mechanism was described for many dimeric and oligomeric protein complexes, where it plays important structural and functional roles (Bennett et al. 1995; van der Wel 2012). It is believed that the increased interaction area between the protein subunits in the complexes formed via the domain swapping mechanism affects the overall protein stability (Bennett et al. 1994; Liu & Eisenberg 2002). In some cases, the formation of the quaternary structure of protein by this mechanism is associated with the emergence of new functions in protein oligomers which are not found in the monomeric forms of these proteins (Liu & Eisenberg 2002). Finally, the domain swapping mechanism is involved in the early stages of the amyloid fibril formation (van der Wel 2012).

Since it is known that the natural environment of a protein inside a living cell is characterized by high concentrations of large biomolecules (other proteins, nucleic acids, ribonucleoproteins, polysaccharides, etc.), in the range of 80–400 mg/ml (Rivas et al. 2004; van den Berg et al. 1999; Zimmerman & Trach 1991) and since this specific milieu is expected to have profound effects on the various biological processes and reactions that depend on the available volume (Minton 2005; Zimmerman & Minton 1993), this work opens a series of articles dedicated to the analysis of the effect of the environmental feature (including the presence of crowding agents) on structural properties and conformational stability of bOBP. In this work, to identify which structural features of bOBP are responsible for the formation of its unique dimeric structure and to understand the role of the domain swapping mechanism in

maintaining the native structure of the protein, structural properties of the recombinant wild type bOBP and its four mutant forms that cannot dimerize via the domain swapping (Ramoni et al. 2008; Ramoni et al. 2002) were analyzed and compared using a spectrum of the biophysical techniques that included intrinsic fluorescence spectroscopy, circular dichroism spectroscopy in the far- and near-UV regions and gel filtration. We also designed two monomeric mutants, GCC-bOBP-W17F and GCC-bOBP-W133F, each containing a single tryptophan residue, for the characterization of the specific features of the microenvironments of these tryptophan residues that affect the intrinsic fluorescence characteristics of this protein.

MATERIALS AND METHODS

Materials

GdnHCl (Nacalai Tesque, Japan) and 1-octen-3-ol (OCT; Sigma-Aldrich, USA) were used without further purification. The protein concentration was 0.1 – 0.2 mg/ml. The OCT concentration was 10 mM. The experiments were performed in 20 mM Na-phosphate-buffered solution at pH 7.8.

Gene expression and protein purification

The plasmids pT7-7-bOBP which encodes recombinant bOBP and its mutant forms with a poly-histidine tag were used to transform *Escherichia coli* BL21(DE3) host (Invitrogen) (Stepanenko et al. 2014b). Protein expression was induced by incubating the cells with 0.3 mM of isopropyl-beta-D-1-thiogalactopyranoside (IPTG; Fluka, Switzerland) for 24 h at 37 °C. The recombinant protein was purified with Ni+-agarose packed in HisGraviTrap columns (GE

Healthcare, Sweden). The protein purity was determined through SDS-PAGE in 15% polyacrylamide gel (Laemmli 1970).

Analyzing the 3D protein structure

We analzed the microenvironment peculiarities for tryptophan residues in the bOBP and GCC-bOBP structure based on PDB data (Dutta et al. 2009) using the 1OBP (Tegoni et al. 1996) and 2HLV PDB files (Ramoni et al. 2008) as described previously (Giordano et al. 2004; Stepanenko et al. 2014a; Stepanenko et al. 2015; Stepanenko et al. 2012; Turoverov et al. 1985).

Fluorescence spectroscopy

Fluorescence experiments were performed using a Cary Eclipse spectrofluorometer (Varian, Australia) with microcells FLR (10 x 10 mm; Varian, Australia). Fluorescence lifetime were measured using a "home built" spectrofluorometer with nanosecond impulse (Turoverov et al. 1998) as well as micro-cells (101.016-QS 5 x 5 mm; Hellma, Germany). Tryptophan fluorescence in the protein was excited at the long-wave absorption spectrum edge (λ_{ex} = 297 nm), wherein the tyrosine residue contribution to the bulk protein fluorescence is negligible. The fluorescence spectra position and form were characterized using the parameter $A = I_{320}/I_{365}$, wherein I_{320} and I_{365} are the fluorescence intensities at the emission wavelengths 320 and 365 nm, respectively (Turoverov & Kuznetsova 2003). The values for parameter A and the fluorescence spectrum were corrected for instrument sensitivity. The tryptophan fluorescence anisotropy was calculated using the equation $r = (I_V^V - GI_H^V)/(I_V^V + 2GI_H^V)$, wherein I_V^V and I_H^V are the vertical and horizontal fluorescence intensity components upon excitement by vertically polarized light. G is the relationship between the fluorescence intensity vertical and horizontal

components upon excitement by horizontally polarized light ($G = I_V^H / I_H^H$), λ_{em} = 365 nm (Turoverov et al. 1998). Protein unfolding was initiated by manually mixing the protein solution (40 µL) with a buffer solution (510 µL) that included the necessary GdnHCl concentration. The GdnHCl concentration was determined by the refraction coefficient using an Abbe refractometer (LOMO, Russia; (Pace 1986)). The dependences of different bOBP fluorescent characteristics on GdnHCl were recorded following protein incubation in a solution with the appropriate denaturant concentration at 4 ºC for 2, 24 and 48 h. bOBP refolding was initiated by diluting the pre-denatured protein (in 3.0 M GdnHCl, 40 µL) with the buffer or denaturant solutions at various concentrations (510 µL). The spectrofluorometer was equipped with a thermostat that holds the temperature constant at 23°C.

Circular dichroism measurements

The CD spectra were generated using a Jasco-810 spectropolarimeter (Jasco, Japan). Far-UV CD spectra were recorded in a 1-mm path length cell from 260 nm to 190 nm with a 0.1 nm step size. Near-UV CD spectra were recorded in a 10-mm path length cell from 320 nm to 250 nm with a 0.1 nm step size. For the spectra, we generated 3 scans on average. The CD spectra for the appropriate buffer solution were recorded and subtracted from the protein spectra.

Gel filtration experiments

We performed gel filtration experiments for bOBP and its mutant forms in a buffered solution without and with addition of GdnHCl using a Superdex-75 PC 3.2/30 column (GE Healthcare, Sweden) and an AKTApurifier system (GE Healthcare, Sweden). The column was equilibrated with the buffered solution or GdnHCl at the desired concentration, and 10 µl of the

protein solution prepared under the same conditions was loaded on the pre-equilibrated column. The change in hydrodynamic dimensions for the studied proteins was evaluated as a change in the bOBP or the mutant protein elution volume. Multiple proteins with known molecular masses (aprotinin (6.5 kDa), ribonuclease (13.7 kDa), carbonic anhydrase (29 kDa), ovalbumin (43 kDa) and conalbumin (75 kDa), which are chromatography standards from GE Healthcare) were used to generate the calibration curve.

Evaluation of the intrinsic disorder predisposition

The intrinsic disorder propensity of the bOBP was evaluated by several disorder predictors, such as PONDR® VLXT (Stepanenko et al. 2015), PONDR® VSL2 (Stepanenko et al. 2014a), PONDR® VL3 (Peng et al. 2006), and PONDR® FIT (Xue et al. 2010). Effects of the point mutations on the intrinsic disorder predisposition of this protein was analyzed by PONDR® VSL2. In these analyses, scores above 0.5 are considered to correspond to the disordered residues/regions. PONDR® VSL2B was chosen for the comparative analysis of the bOBP mutants since this tool is one of the more accurate stand-alone disorder predictors (Fan & Kurgan 2014; Peng & Kurgan 2012; Stepanenko et al. 2014a), PONDR® VLXT is known to have high sensitivity to local sequence peculiarities and can be used for identifying disorder-based interaction sites (Stepanenko et al. 2015), PONDR® VL3 provides accurate evaluation of long disordered regions (Peng et al. 2006), whereas a metapredictor PONDR-FIT is moderately more accurate than each of the component predictors, PONDR® VLXT (Stepanenko et al. 2015), PONDR® VSL2 (Stepanenko et al. 2014a), PONDR® VL3 (Peng et al. 2006), FoldIndex (Prilusky et al. 2005), IUPred (Dosztanyi et al. 2005), TopIDP (Campen et al. 2008). PONDR-FIT (Xue et al. 2010).

RESULTS AND DISCUSSION

It is believed that the introduction of an extra glycine residue after the bOBP residue 121 (Figure 2) should result in the increased mobility of the loop connecting α-helix and 8th β-strand of the β-barrel, which, in its turn, promotes the formation of a monomeric fold of the mutant protein bOBP-Gly121+. Substitutions of the residues Trp64 and His156 to cysteines in bOBP-Gly121+ generate a mutant form GCC-bOBP, which should have stable monomeric structure due to the restoration of the disulfide bond typically seeing in classical OBPs. Finally, to characterize specific features of the microenvironments of tryptophan residues W17 and W133 that might affect the intrinsic fluorescence of the protein, we designed two monomeric mutant forms GCC-bOBP-W17F and GCC-bOBP-W133F, each containing a single tryptophan residue.

To evaluate potential effects of selected mutations on protein structure, we analyzed substitution-induced changes in the intrinsic disorder propensity of bOBP. It has been pointed out that such computational analysis can provide useful information on the expected outcomes of the point mutations in proteins (Melnik et al. 2012; Moroz et al. 2013; Uversky et al. 2011; Vacic et al. 2012). Figure 3A represents the results of the multi-tool analysis of the per-residue intrinsic disorder predisposition of bOBP. We used here several members of the PONDR family, PONDR® VLXT (Stepanenko et al. 2015), PONDR® VSL2 (Stepanenko et al. 2014a), and PONDR® FIT (Xue et al. 2010). Figure 3A shows that all these tools are generally agree with each other and indicates that although bOBP is predicted to be mostly ordered, this protein possesses several disordered or flexible regions. Disordered regions are defined here as protein fragments containing residues with the disorder scores above the 0.5 threshold, whereas regions

are considered flexible if disorder scores of their residues ranges from 0.3 to 0.5. Figure 3B represents the results of the disorder evaluation in mutant forms of the bOBP and shows the aligned PONDR® VSL2-based disorder profiles for the wild type protein and its four mutants. These analyses revealed that the wild type bOBP and its four mutants are expected to be rather ordered (clearly belonging to the category of hybrid proteins that contain ordered domains and intrinsically disordered regions) and that mutations do not induce significant changes in the bOBP disorder propensity.

Previously, we have shown that the recombinant bOBP, unlike native bOBP purified from the tissue, exists in a stable native-like state as a mixture of monomeric and dimeric forms (Stepanenko et al. 2014b) (Figure 4, Table 1). Furthermore, the recombinant bOBP forms dimers in the presence of relatively high denaturant concentrations (e.g., in a solution of 1.5 M guanidine hydrochloride, GdnHCl). The dimerization process is accompanied by the formation of a stable, more compact, intermediate state maximally populated at 0.5M GdnHCl.

In the present work, gel filtration analysis revealed that all investigated mutants of the bOBP, namely bOBP-Gly121+, GCC-bOBP, GCC-bOBP-W17F, and GCC-bOBP-W133F, are monomers (Figure 5, Table 1). The positions of the elution peaks of the studied mutant bOBP forms coincided with the positions of the elution peak of the monomeric form of recombinant bOBP. This indicates that the amino acid substitutions introduced to the bOBP sequence did not affect the compact structure of this protein.

Investigation of the interaction of recombinant bOBP with its natural ligand 1-Octen-3-ol (OCT) by gel-filtration chromatography revealed that the elution profile of the bOBP/OCT complex contained two peaks (Figure 5). These data indicate that similar to the recombinant bOBP the bOBP/OCT complex exists as a mixture of monomeric and dimeric forms of the

protein. However, the positions of the two peaks in the bOBP/OCT elution profile are shifted to slightly higher elution volume, suggesting that the OCT binding induces partial compaction of both the monomeric and dimeric forms of the protein. Figure 5 shows that all mutants also gained more compact conformation in the presence of OCT, illustrating that the introduced mutations do not affect functional activity of the bOBP and its ability to bind a natural ligand.

Table 1 and Figure 6 shows that the recombinant bOBP is characterized by a relatively long-wave position of the intrinsic tryptophan fluorescence (λ_{max} = 335 nm at λ_{ex} = 297 nm). The intrinsic fluorescence of bOBP is determined by three tryptophan residues, two of which are located in the β-sheet (Trp17 is in the first β-strand, and Trp64 is in the fourth β-strand), whereas Trp133 is included into a single α-helix of this protein. Among all the tryptophan residues of the protein Trp133 has the lowest density of the microenvironment (d = 0.54), indicating that it is partially accessible to the solvent (Table 2). The microenvironments of Trp16 and Trp64 are more dense (0.80 and 0.71, respectively), but also more polar compared with the Trp133 local environment (Tables 2-5).

It should be noted that the side chains of the charged residues Lys121 and Lys59 included in the microenvironments of Trp17 and Trp64, respectively, are oriented parallel to the indole ring of the corresponding tryptophan residue, and their NZ amino groups are located at a short distance from NE1 group of the corresponding tryptophan residue (5.16 and 4.55 Å for NZ groups Lys121 and Lys59, Tables 3-4). Therefore, the presence of a partial fluorescence quenching of Trp17 and Trp64 cannot be excluded, since fluorescence quenching was previously reported for a single tryptophan residue Trp16 of porcine OBP that has similar features in its microenvironment (Staiano et al. 2007; Stepanenko et al. 2008).

Recombinant bOBP is characterized by high values of fluorescence anisotropy and fluorescence lifetime (Table 1), and also has a pronounced CD spectrum in the near-UV region (Figure 7). These observations indicate that the environment of tryptophan residues of this protein is quite rigid and asymmetric.

The monomeric bOBP-Gly121+ is characterized by a somewhat longer wavelength of the tryptophan fluorescence spectrum and lower value of the fluorescence anisotropy compared to the recombinant bOBP (Table 1, Figure 6). The near-UV CD spectrum of the bOBP-Gly121+ is almost indistinguishable for the spectrum of recombinant bOBP (Figure 7). This indicates that although the overall spatial structure of the protein is not perturbed by adding an extra Gly residue after the position 121, the local microenvironment of the tryptophan residues become less dense due to this sequence perturbation. Importantly, the magnitudes of the fluorescence lifetime and fluorescence quantum yield of the bOBP-Gly121+ are higher than those for the recombinant bOBP. It is likely that the more mobile microenvironments of the tryptophan residues in bOBP-Gly121+ might result in the removal of some potential quenching groups from the indole ring of these tryptophan residues, thereby leading to a weakening of the quenching effects.

The values of the fluorescence parameters such as the position of the maximal tryptophan fluorescence, fluorescence anisotropy, and fluorescence lifetime for the triple mutant GCC-bOBP, which was designed to have disulfide bond via substituting residues Trp64 and His156 of the bOBP-Gly121+ to the cysteine residues, were similar to these parameters recorded for the recombinant bOBP (Table 1, Figure 6). The intensity of the negative band in the near-UV CD spectrum of the GCC-bOBP variant was greater than that of the recombinant bOBP (Figure 7). These data demonstrate the stabilizing effect of the disulfide bond to the protein structure. The intensity of the GCC-bOBP tryptophan fluorescence was approximately 25% lower than that of

the recombinant bOBP (Figure 6). Since the structure of the GCC-bOBP retained only two of the three tryptophan residues of the protein, namely Trp17 and Trp133, it can be argued that the removed residue Trp64 made a significant contribution to the fluorescence of recombinant bOBP.

Mutant forms designed to have a single tryptophan residue, GCC-bOBP-W17F (contains only Trp133) and the GCC-bOBP-W133F (contains only Trp17) are characterized by the substantially different parameters of tryptophan fluorescence and near-UV CD spectra (Figures 6 and 7). These data indicate that the microenvironments of the residues Trp17 and Trp133 are significantly different from each other. It should be noted that the calculated total spectrum of the intrinsic fluorescence of these two proteins GCC-bOBP-W17F and GCC-bOBP-W133F (calculated as a weighted sum of individual spectra) coincides with the tryptophan fluorescence spectrum of GCC-bOBP (Figure 6). These data together with the results of the gel filtration analysis suggested that the mutant proteins GCC-bOBP-W17F and GCC-bOBP-W133F maintained native-like, mostly unperturbed spatial structures, and that the microenvironments of their residues Trp17 and Trp133 are similar to the environments of these residues in the GCC-bOBP protein.

The position of the tryptophan fluorescence spectrum of the GCC-bOBP-W17F mutant, and the values of its parameter A, fluorescence anisotropy, and fluorescence lifetime suggest that the microenvironment of the Trp133 residue is relatively polar and mobile, and the residue itself contributes significantly to the total fluorescence of this protein (Table 1). These data agree well with the results of the analysis of the specific characteristics of the microenvironment of tryptophan residues in the wild type bOBP (Tables 2-5) and the GCC-bOBP mutant (Tables 2-5). At the same time, the spectral characteristics of the GCC-bOBP-W133F mutant suggest that the

Trp17 can be considered as an internal residue located within a very dense, inaccessible to solvent microenvironment. Furthermore, the fluorescence of this residue is substantially quenched (Table 1, Figure 6).

Analysis of the microenvironment of tryptophan residues in the wild type bOBP and its GCC-bOBP mutant suggests that the Trp17 residues is substantially quenched by the Lys121 which is included into the Trp17 microenvironment and is oriented parallel to the indole ring of the tryptophan residue (Staiano et al. 2007) (Table 3). However, as aforementioned, the Trp64 residue, which also has a lysine residue (Lys59) in its microenvironment with the conformation similar to that of Lys121, makes a significant contribution to the total fluorescence of the recombinant bOBP (Figure 8). We suggest this is due to the fact that the direct interaction of the Lys59 nitrogen with the indole ring of Trp64 is screened by a water molecule, which is in the direct contact with the nitrogen atom of the Trp64 indole ring (Figure 8).

The far-UV CD spectra recorded for the recombinant bOBP and its four mutant forms (bOBP-Gly121+, GCC-bOBP, GCC-bOBP-W17F, and GCC-bOBP-W133F) are rather similar and have a shape characteristic of protein enriched in the β-structural elements (Figure 9). Decomposition of the far-UV CD spectrum of the recombinant bOBP using the Provencher's algorithm (Provencher & Glockner 1981) revealed that this protein contains 13% α-helix, 36% β-sheet, and 20% β-turns (Table 6). These data agree well with the results of the X-ray analysis of the wild type bOBP (13% α-helix and 46% β-sheets). In the bOBP-Gly121+, adding the Gly121+ insert leads to a certain decrease in the content of α-helical elements (Table 6). Obviously, the insertion of an extra Gly121 residue to the loop segment preceding the single α-helix of the protein reduces the length of this helical element. On the other hand, the introduction of a disulfide bond to the structure of the triple mutant GCC-bOBP leads to a full recovery of the

protein secondary structure, confirming the stabilizing effects of the disulfide bond in the monomeric form of the protein. Replacement of the tryptophan residue Trp133 to phenylalanine in the mutant form GCC-bOBP-W133F leads to an increase in the content of α-helical elements. It is likely that the substitution of a balky tryptophan residue by a less massive residue in the single α-helix of this protein reduces some steric constraints during the α-helix formation and increases length of the helical element. In contrast, in mutant form GCC-bOBP-W17F, replacement of a tryptophan residue Trp17 to phenylalanine leads to a marked decrease in α-helical structure and increase in β-sheet structure. Perhaps, the absence of the bulky Trp17 in the first β-sheet of the β-barrel favors the formation of a closer contact between the β-strands of the protein's β-barrel.

In the presence of the OCT ligand, the fluorescent characteristics and the near- and far-UV CD spectra of the recombinant bOBP and its mutant forms undergo significant changes, indicating compaction and stabilization of the spatial structure of these proteins (Tables 1 and 6). These data also suggest that all mutant forms of bOBP analyzed in this work retain the ability to bind a natural ligand.

Therefore, all mutant forms of bOBP generally retain tertiary and secondary structure. Their structural organization is rather similar to that of the recombinant bOBP. The structure of the GCC-bOBP is closest to the structure of the recombinant wild type bOBP. The observed changes in the local structure of the mutant forms of bOBP do not violate the ability of the protein to correctly fold and bind a natural ligand. Ligand binding to the bOBP mutant forms leads to a more compact state of the studied proteins and does not alter its oligomeric status.

CONCLUSIONS

We show here that the insertion of Gly121+ leads to disruption of the domain swapping mechanism, resulting in a stable monomeric mutant protein bOBP-Gly121+. The introduction of a disulfide bond induces noticeable stabilization of the monomeric fold of the GCC-bOBP mutant. The amino acid substitutions introduced to bOBP in this study, such as Gly121+ insertion in the bOBP-Gly121+ mutant, replacement of the Trp64 and His156 to the cysteine residues in the GCC-bOBP mutant, and replacement of the Trp17 and Trp133 residues to phenylalanine in the GCC-bOBP-W17F and GCC-bOBP-W133F mutants, do not disrupt the functional activity of the protein. We show that the ligand binding leads to the formation of a more compact and stable state of the recombinant bOBP and its mutant monomeric forms. We also describe the peculiarities of the microenvironment of tryptophan residues of the protein which are essential for the formation of the fluorescent properties of the protein and which were not described previously.

ACKNOWLEDGEMENTS

This work was supported by a grant from the Russian Science Foundation RSCF № 14-24-00131 (KKT).

AUTHOR CONTRIBUTIONS

Olga VS, Olesya VS and DOR collected and analyzed data, contributed to discussion, and wrote the manuscript. IMK and KKT conceived the idea, supervised the project, contributed to discussion, and reviewed/edited manuscript. VNU analyzed data, contributed to discussion, and wrote the manuscript.

DISCLOSURE

None declared.

REFERENCES

Bennett MJ, Choe S, and Eisenberg D. 1994. Domain swapping: entangling alliances between proteins. *Proc Natl Acad Sci U S A* 91:3127-3131.

Bennett MJ, Schlunegger MP, and Eisenberg D. 1995. 3D domain swapping: a mechanism for oligomer assembly. *Protein Sci* 4:2455-2468.

Bianchet MA, Bains G, Pelosi P, Pevsner J, Snyder SH, Monaco HL, and Amzel LM. 1996. The three-dimensional structure of bovine odorant binding protein and its mechanism of odor recognition. *Nat Struct Biol* 3:934-939.

Campen A, Williams RM, Brown CJ, Meng J, Uversky VN, and Dunker AK. 2008. TOP-IDP-scale: a new amino acid scale measuring propensity for intrinsic disorder. *Protein Pept Lett* 15:956-963.

Dosztanyi Z, Csizmok V, Tompa P, and Simon I. 2005. IUPred: web server for the prediction of intrinsically unstructured regions of proteins based on estimated energy content. *Bioinformatics* 21:3433-3434.

Dutta S, Burkhardt K, Young J, Swaminathan GJ, Matsuura T, Henrick K, Nakamura H, and Berman HM. 2009. Data deposition and annotation at the worldwide protein data bank. *Mol Biotechnol* 42:1-13.

Fan X, and Kurgan L. 2014. Accurate prediction of disorder in protein chains with a comprehensive and empirically designed consensus. *J Biomol Struct Dyn* 32:448-464.

Flower DR, North AC, and Sansom CE. 2000. The lipocalin protein family: structural and sequence overview. *Biochim Biophys Acta* 1482:9-24.

Giordano A, Russo C, Raia CA, Kuznetsova IM, Stepanenko OV, Turoverov KK, Stepanenko OV, Kuznetsova IM, Turoverov KK, Huang C, and Wang CC. 2004. Highly UV-absorbing complex in selenomethionine-substituted alcohol dehydrogenase from Sulfolobus solfataricus

Conformational change of the dimeric DsbC molecule induced by GdnHCl. A study by intrinsic fluorescence. *J Proteome Res* 3:613-620.

Hsin J, Arkhipov A, Yin Y, Stone JE, and Schulten K. 2008. Using VMD: an introductory tutorial. *Curr Protoc Bioinformatics* Chapter 5:Unit 5 7.

Laemmli UK. 1970. Cleavage of structural proteins during the assembly of the head of bacteriophage T4. *Nature* 227:680-685.

Liu Y, and Eisenberg D. 2002. 3D domain swapping: as domains continue to swap. *Protein Sci* 11:1285-1299.

Melnik BS, Povarnitsyna TV, Glukhov AS, Melnik TN, Uversky VN, and Sarma RH. 2012. SS-Stabilizing Proteins Rationally: Intrinsic Disorder-Based Design of Stabilizing Disulphide Bridges in GFP. *J Biomol Struct Dyn* 29:815-824.

Merritt EA, and Bacon DJ. 1977. Raster3D: Photorealistic molecular graphics. . *Methods enzymol* 277:505-524.

411 Minton AP. 2005. Models for excluded volume interaction between an unfolded protein and
412 rigid macromolecular cosolutes: macromolecular crowding and protein stability revisited.
413 *Biophys J* 88:971-985.
414 Moroz NA, Novak SM, Azevedo R, Colpan M, Uversky VN, Gregorio CC, and Kostyukova AS.
415 2013. Alteration of tropomyosin-binding properties of tropomodulin-1 affects its capping
416 ability and localization in skeletal myocytes. *J Biol Chem* 288:4899-4907.
417 Pace CN. 1986. Determination and analysis of urea and guanidine hydrochloride denaturation
418 curves. *Methods Enzymol* 131:266-280.
419 Peng K, Radivojac P, Vucetic S, Dunker AK, and Obradovic Z. 2006. Length-dependent
420 prediction of protein intrinsic disorder. *BMC Bioinformatics* 7:208.
421 Peng ZL, and Kurgan L. 2012. Comprehensive comparative assessment of in-silico predictors of
422 disordered regions. *Curr Protein Pept Sci* 13:6-18.
423 Prilusky J, Felder CE, Zeev-Ben-Mordehai T, Rydberg EH, Man O, Beckmann JS, Silman I, and
424 Sussman JL. 2005. FoldIndex: a simple tool to predict whether a given protein sequence
425 is intrinsically unfolded. *Bioinformatics* 21:3435-3438.
426 Provencher SW, and Glockner J. 1981. Estimation of globular protein secondary structure from
427 circular dichroism. *Biochemistry* 20:33-37.
428 Ramoni R, Spinelli S, Grolli S, Conti V, Merli E, Cambillau C, and Tegoni M. 2008.
429 Deswapping bovine odorant binding protein. *Biochim Biophys Acta* 1784:651-657.
430 Ramoni R, Vincent F, Ashcroft AE, Accornero P, Grolli S, Valencia C, Tegoni M, and
431 Cambillau C. 2002. Control of domain swapping in bovine odorant-binding protein.
432 *Biochem J* 365:739-748.
433 Rivas G, Ferrone F, and Herzfeld J. 2004. Life in a crowded world. *EMBO Rep* 5:23-27.
434 Spinelli S, Ramoni R, Grolli S, Bonicel J, Cambillau C, and Tegoni M. 1998. The structure of
435 the monomeric porcine odorant binding protein sheds light on the domain swapping
436 mechanism. *Biochemistry* 37:7913-7918.
437 Staiano M, D'Auria S, Varriale A, Rossi M, Marabotti A, Fini C, Stepanenko OV, Kuznetsova
438 IM, and Turoverov KK. 2007. Stability and dynamics of the porcine odorant-binding
439 protein. *Biochemistry* 46:11120-11127.
440 Stepanenko OV, Bublikov GS, Stepanenko OV, Shcherbakova DM, Verkhusha VV, Turoverov
441 KK, and Kuznetsova IM. 2014a. A knot in the protein structure - probing the near-
442 infrared fluorescent protein iRFP designed from a bacterial phytochrome. *Febs J*
443 281:2284-2298.
444 Stepanenko OV, Fonin AV, Stepanenko OV, Staiano M, D'Auria S, Kuznetsova IM, and
445 Turoverov KK. 2015. Tryptophan residue of the D-galactose/D-glucose-binding protein
446 from E. Coli localized in its active center does not contribute to the change in intrinsic
447 fluorescence upon glucose binding. *J Fluoresc* 25:87-94.
448 Stepanenko OV, Marabotti A, Kuznetsova IM, Turoverov KK, Fini C, Varriale A, Staiano M,
449 Rossi M, and D'Auria S. 2008. Hydrophobic interactions and ionic networks play an
450 important role in thermal stability and denaturation mechanism of the porcine odorant-
451 binding protein. *Proteins* 71:35-44.
452 Stepanenko OV, Stepanenko OV, Kuznetsova IM, Shcherbakova DM, Verkhusha VV, and
453 Turoverov KK. 2012. Distinct effects of guanidine thiocyanate on the structure of
454 superfolder GFP. *PLoS One* 7:e48809.

455 Stepanenko OV, Stepanenko OV, Staiano M, Kuznetsova IM, Turoverov KK, and D'Auria S.
456 2014b. The quaternary structure of the recombinant bovine odorant-binding protein is
457 modulated by chemical denaturants. *PLoS One* 9:e85169.
458 Tegoni M, Pelosi P, Vincent F, Spinelli S, Campanacci V, Grolli S, Ramoni R, and Cambillau C.
459 2000. Mammalian odorant binding proteins. *Biochim Biophys Acta* 1482:229-240.
460 Tegoni M, Ramoni R, Bignetti E, Spinelli S, and Cambillau C. 1996. Domain swapping creates a
461 third putative combining site in bovine odorant binding protein dimer. *Nat Struct Biol*
462 3:863-867.
463 Turoverov KK, Biktashev AG, Dorofeiuk AV, and Kuznetsova IM. 1998. [A complex of
464 apparatus and programs for the measurement of spectral, polarization and kinetic
465 characteristics of fluorescence in solution]. *Tsitologiia* 40:806-817.
466 Turoverov KK, and Kuznetsova IM. 2003. Intrinsic fluorescence of actin. *J Fluorescence* 13:41-
467 57.
468 Turoverov KK, Kuznetsova IM, and Zaitsev VN. 1985. The environment of the tryptophan
469 residue in Pseudomonas aeruginosa azurin and its fluorescence properties. *Biophys Chem*
470 23:79-89.
471 Uversky VN, Shah SP, Gritsyna Y, Hitchcock-DeGregori SE, and Kostyukova AS. 2011.
472 Systematic analysis of tropomodulin/tropomyosin interactions uncovers fine-tuned
473 binding specificity of intrinsically disordered proteins. *J Mol Recognit* 24:647-655.
474 Vacic V, Markwick PR, Oldfield CJ, Zhao X, Haynes C, Uversky VN, and Iakoucheva LM.
475 2012. Disease-associated mutations disrupt functionally important regions of intrinsic
476 protein disorder. *PLoS Comput Biol* 8:e1002709.
477 van den Berg B, Ellis RJ, and Dobson CM. 1999. Effects of macromolecular crowding on
478 protein folding and aggregation. *EMBO J* 18:6927-6933.
479 van der Wel PC. 2012. Domain swapping and amyloid fibril conformation. *Prion* 6:211-216.
480 Xue B, Dunbrack RL, Williams RW, Dunker AK, and Uversky VN. 2010. PONDR-FIT: a meta-
481 predictor of intrinsically disordered amino acids. *Biochim Biophys Acta* 1804:996-1010.
482 Zimmerman SB, and Minton AP. 1993. Macromolecular crowding: biochemical, biophysical,
483 and physiological consequences. *Annu Rev Biophys Biomol Struct* 22:27--65.
484 Zimmerman SB, and Trach SO. 1991. Estimation of macromolecule concentrations and excluded
485 volume effects for the cytoplasm of Escherichia coli. *J Mol Biol* 222:599--620.
486
487

FIGURE LEGENDS

Figure 1. 3D structure of bOBP. The individual subunits in the protein are in gray and orange. The tryptophan residues in the different subunits are indicated in red and blue. The Lys 121 residue after which an extra glycine residue are inserted in the mutant form bOBP-Gly121+ is drown in green. Additionally the residues Trp 64 and His 156 (yellow) are substituted for cysteine in the mutant form GCC-bOBP. The drawing was generated based on the 1OBP file (Tegoni et al. 1996) from PDB (Dutta et al. 2009) using the graphic software VMD (Hsin et al. 2008) and Raster3D (Merritt & Bacon 1977).

Figure 2. Sequence peculiarities of various bPDB forms. The comparison of the primary sequence for the recombinant bOBPwt and its mutant forms bOBP-Gly121+ and GCC- bOBP, which are not able to form domain-swapped dimers. The mutant forms GCC-bOBP-W17F and GCC-bOBP-W133F designed to contain a single tryptophan residue were produced to investigate the peculiarities of the microenvironment of the tryptophan residues.

Figure 3. Intrinsic disorder propensity of the wild type bOBP and its mutants. **A**. Per-residue disorder propensity of the wild type bOBP evaluated by members of the PONDR family, PONDR® VLXT (Stepanenko et al. 2015) (green line), PONDR® VSL2 (Stepanenko et al. 2014a) (blue line), PONDR® FIT (Xue et al. 2010) (red line) and PONDR® VL3 (pink line). Localization of known elements of the bOBP secondary structure is shown by colored bars at the bottom of the plot. Light pink shadow around the PONDR® FIT curve represents distribution of

errors in the disorder score evaluation. **B**. Effects of mutations on the intrinsic disorder propensity of bOBP evaluated by PONDR® VSL2.

Figure 4. GdnHCl-induced conformational changes in bOBP (data for this figure are taken from (Stepanenko et al. 2014b)). **A**. changes in fluorescence intensity at 320 nm, λ_{ex}=297 nm; **B**. changes in parameter *A*, λ_{ex}=297 nm; **C**. changes in fluorescence anisotropy at the emission wavelength 365 nm, λ_{ex}=297 nm; **D**. changes in the ellipticity at 222 nm. The measurements were preceded by incubating the protein in a solution with the appropriate GdnHCl concentration at 4ºC for 24 h. The open symbols indicate unfolding, whereas the closed symbols represent refolding. Changes in bOBP hydrodynamic dimensions for the different structural states were followed by the changes in the elution profiles for bOBP after pre-incubation for 24 h (solid lines) and 43 h (dashed line) with GdnHCl at the concentrations 0.0 (**E**), 0.5 (**F**) and 1.5 (**G**) for the denaturation process.

Figure 5. Hydrodynamic characteristics of the bOBP and its mutants. The changes of hydrodynamic dimensions of recombinant bOBP (1) and its mutant forms bOBP-Gly121+ (2), GCC-bOBP (3), GCC-bOBP-W17F (4) and GCC-bOBP-W133F (5) in the absence (solid lines) and the presence of OCT (dotted lines).

Figure 6. Tertiary structure changes for bOBP (red) and its mutant forms bOBP-Gly121+ (green), GCC-bOBP (blue), GCC-bOBP-W17F (gray) and GCC-bOBP-W133F (dark yellow) in different structural states as indicated by intrinsic tryptophan fluorescence (λ_{ex}=297 nm). The spectra shown are for the protein in buffered solution (solid line), in the presence of

natural ligand OCT (dotted line) and in the presence of 3.5 M GdnHCl (dashed line). The corresponding spectra in light blue were obtained as a sum of the spectra for GCC-bOBP-W17F and GCC-bOBP-W133F.

Figure 7. Tertiary structure for bOBP (red) and its mutant forms bOBP-Gly121+ (green), GCC-bOBP (blue), GCC-bOBP-W17F (gray) and GCC-bOBP-W133F (dark yellow) in buffered solution as indicated by near-UV CD spectra. The spectrum in light blue was obtained as a sum of the spectra for GCC-bOBP-W17F and GCC-bOBP-W133F.

Figure 8. The microenvironment of Trp 17 (*A*) and Trp 64 (*B*) in bOBP. The spatial orientation of lysine residues relative the indole ring of tryptophan residues is shown. The drawing was generated based on the 1OBP file (Tegoni et al. 1996) from PDB (Dutta et al. 2009) using the graphic software VMD (Hsin et al. 2008) and Raster3D (Merritt & Bacon 1977).

Figure 9. Secondary structure for bOBP (red) and its mutant forms bOBP-Gly121+ (green), GCC-bOBP (blue), GCC-bOBP-W17F (gray) and GCC-bOBP-W133F (dark yellow) in buffered solution as indicated by far-UV CD spectra.

Table 1(on next page)

Tables

Table 1. Characteristics of recombinant bOBPwt and its mutant forms in different structural states as well as in the presence of natural ligand OCT.

	Intrinsic fluorescence				*Hydrodynamic dimensions*	
	λ_{max}, nm[1]	Par *A*[1]	r^2	<τ>, ns[3]	1 peak, kDa	2 peak, kDa
bOBPwt (*in buffered solution*)[4]	335	1,21	0,170	4.37 ± 0.19	43.9	23.8
bOBPwt (*in 0.5 M GdnHCl - I_1 state*)[4]	337	1,10	0,166	4.62±0.19	34.0	19.3
bOBPwt (*in 1.6 M GdnHCl – I_2 state*)[4]	335	1,20	0,180	4.76±0.10	43.6	
bOBPwt/OCT	334	1,30	0,177		39.6	21.5
bOBPwt in 3.5 M GdnHCl	349	0,47	0,062			
bOBP/Gly121+	336	1,13	0,166	4,63 ± 0.06	23.6	
bOBP/Gly121+/OCT	335	1,12	0,170		21.5	
bOBP/Gly121+ in 3.5 M GdnHCl	350	0,47	0,059			
GCC-bOBP	335	1,05	0,170	4,30 ± 0.16	23.6	
GCC-bOBP/OCT	335	1,05	0,174		22.5	
GCC-bOBP in 3.5 M GdnHCl	348	0,48	0,060			
GCC-bOBP-W17F	339	0,82	0,164	4,67 ± 0.13	23.6	
GCC-bOBP-W17F/OCT	339	0,82	0,165		22.5	
GCC-bOBP-W17F in 3.5 M GdnHCl	349	0,49	0,066			
GCC-bOBP-W133F	325	2,83	0,186	1,89 ± 0.40	23.6	
GCC-bOBP-W133F/OCT	323	3,02	0,189		23.6	
GCC-bOBP-W133F in 3.5 M GdnHCl	350	0,46	0,056			

[1] λ_{ex} = 297 nm;

[2] λ_{ex}=297 nm, λ_{em}=365 nm;

[3] λ_{ex}=297 nm, λ_{em}=335 nm

[4] The data are from [1]

Table 2. Side chain conformation of Trp residues in bOBPwt and GCC-bOBP.

Protein	Residue	N (*d*)*	χ_1, (deg)*	χ_2, (deg)*
bOBPwt	Trp 17	84 (0.80)	283.18	78.87
	Trp 64	80 (0.71)	278.04	99.85
	Trp 133	56 (0.54)	287.95	112.22
GCC-bOBP	Trp 17	87 (0.83)	292.40	82.09
	Trp 133	48 (0.50)	283.53	103.91

* N is the number of atoms in the microenvironment of tryptophan residue; *d* is the density of tryptophan residue microenvironment; χ_1 and χ_2 are the angles characterizing the conformation of tryptophan residue side chain.

32 **Table 3**. Characteristics of the Trp 17 microenvironment in bOBPwt.
33

bOBPwt			GCC-bOBP		
residue	atom	R*, Å	residue	atom	R*, Å
		polar groups			
Ser 14	OG(NE1)	6.86	Ser 14	OG(NE1)	6.61
Arg 18	NE(O)	4.16	Arg 18	NH1(C)	6.17
Arg 18	NH1(O)	2.95	Arg 18	NE(C)	6.46
Arg 18	NH2(O)	5.18	Thr 19	OG1(O)	6.16
Glu 42	OE1(N)	5.44	Arg 41	NH1(O)	6.26
Glu 42	OE2(N)	6.15	Ser 95	OG(CH2)	6.02
Ser 95	OG(CH2)	6.67	Thr 97	OG1(CH2)	6.78
His 98	ND1(CZ3)	6.87	His 98	ND1(CZ3)	6.75
Lys 121	NZ (NE1)	5.16	Lys 121	NZ (NE1)	4.83
HOH 318A	(CZ3)	6.87	HOH 1006	(O)	4.90
			HOH 1047	(C)	4.33
			HOH 1066	(N)	5.20
			HOH 1080	(CD1)	6.62
			HOH 1107	(O)	6.46
		peptide bonds			
Leu 13	O(NE1)	2.87	Leu 13	O(NE1)	2.74
Ser 14	O(NE1)	5.05	Glu 12	O(NE1)	6.62
Ser 14	N(NE1)	4.86	Ser 14	O(NE1)	5.11
Gly 15	O(N)	3.66	Ser 14	N(NE1)	4.74
Gly 15	N(NE1)	4.43	Gly 15	O(N)	3.08
Pro 16	N(N)	3.54	Gly 15	N(CD1)	4.19
Pro 16	O(N)	2.25	Pro 16	N(N)	3.15
Arg 18	N(C)	1.32	Pro 16	O(N)	2.21
Arg 18	O(C)	3.95	Arg 18	N(C)	1.33
Phe 40	O(O)	3.26	Arg 18	O(C)	3.93
Phe 40	N(O)	5.10	Thr 19	N(C)	4.49
Glu 42	N(O)	4.22	Thr 19	O(C)	6.91
Glu 42	O(CD1)	5.73	Tyr 39	O(O)	6.37
Leu 43	N(CD1)	4.02	Phe 40	O(O)	3.24
Leu 43	O(CD1)	4.49	Phe 40	N(O)	5.11
Ser 95	O(CH2)	4.14	Arg 41	N(O)	3.64
Ser 95	N(CH2)	5.77	Arg 41	O(O)	3.53
Arg 96	N(CH2)	4.71	Glu 42	N(O)	4.07
Arg 96	O(CH2)	6.11	Glu 42	O(CB)	5.54
Thr 97	N(CH2)	5.09	Leu 43	N(CD1)	3.86
Thr 97	O(CZ3)	3.76	Leu 43	O(CD1)	4.44
His 98	O(CH2)	4.10	Val 44	N(CD1)	6.03
His 98	N(CZ3)	4.14	Tyr 55	O(O)	5.97
Leu 99	N(CZ3)	3.74	Ser 95	O(CH2)	3.55
Leu 99	O(CZ3)	5.57	Ser 95	N(CH2)	5.32
Phe 119	O(CZ3)	3.85	Arg 96	N(CH2)	5.48
Phe 119	N(CE3)	5.75	Arg 96	O(CZ2)	4.43
Val 120	O(CA)	3.38	Thr 97	N(CH2)	4.59
Val 120	N(CE3)	3.92	Thr 97	O(CZ3)	4.10
Lys 121	O(CA)	6.07	His 98	O(CH2)	3.67
Lys 121	N(CE3)	3.51	His 98	N(CH2)	3.82
Leu 122	N(CA)	4.61	Leu 99	N(CZ3)	3.64
Leu 122	O(O)	5.97	Leu 99	O(CZ3)	5.59
			Val 100	N(CZ3)	6.72

			Phe 119	O(CZ3)	3.53
			Phe 119	N(CE3)	5.67
			Val 120	O(CA)	3.51
			Val 120	N(CE3)	3.73
			Lys 121	O(CD2)	6.58
			Lys 121	N(CE3)	3.77
			Gly 121+	N(CZ3)	6.22
nonpolar groups and aromatic residues					
Pro 16	**CB**, CG, CD	3.49	Pro 16	**CB**, CG, CD	3.73
Phe 40	**CB**, CG, CD1, CD2,CE2	3.74	Phe 40	**CB**, CG, CD1, CD2,CE1	3.72
Phe 45	CG, CD1, **CE1**, CE2, CZ	4.61	Phe 45	CG, CD1, CD2, **CE1**, CE2, CZ	4.06
His 98	**CB**, CG	5.32	His 98	**CB**, CG, CD2	5.18
Phe 119	**CB**, CG, CD1, CD2	4.13	Phe 119	**CB**, CG, CD1, CD2	4.08
Leu 13	CB, CG, CD1, **CD2**	4.17	Leu 13	**CB**, CG, CD1, CD2	4.65
Leu 43	**CB**, CG, CD1, CD2	3.65	Leu 43	**CB**, CG, CD1, CD2	3.52
Leu 94	CB, CG, **CD1**, CD2	4.26	Leu 94	CB, CG, **CD1**, CD2	4.37
Leu 99	**CB**, CG, CD1, CD2	3.80	Leu 99	**CB**, CG, CD1, CD2	3.75
Val 120	**CB**, CG1, CG2	5.51	Val 120	**CB**, CG1, CG2	5.26
Lys 121	**CB**, CG, CD, CE	3.83	Lys 121	CB, CG, **CD**, CE	3.61
Leu 122	CB**,** CG, **CD1**, CD2	4.69			

*R is the minimal distance between a residue involved in the microenvironment of tryptophan residue and its indole ring.

Table 4. Characteristics of the Trp 64 microenvironment in bOBPwt.

residue	atom	R*, Å
	polar groups	
Tyr 39	OH(CH2)	5.35
Ser 57	OG(CE3)	5.05
Lys 59	NZ(NE1)	4.55
Lys 63	NZ(N)	6.58
Lys 65	NZ(O)	5.23
His 157	ND1(CD1)	3.27
His 157	NE2(CD1)	4.22
Glu 159	OE1(CH2)	5.16
Glu 159	OE2(CH2)	4.56
HOH 205A	(CH2)	4.04
HOH 231A	(CZ3)	5.70
HOH 247A	(CH2)	5.80
HOH 282A	(CD2)	3.74
HOH 289A	(CB)	4.18
HOH 298A	(CZ3)	3.56
HOH 328A	(NE1)	2.88
	peptide bonds	
Tyr 39	N(CZ3)	6.04
Tyr 39	O(CZ3)	6.78
Ser 57	N(CZ3)	5.96
Ser 57	O(CZ3)	4.20
Val 58	N(CE3/CZ3)	4.00
Val 58	O(C)	3.67
Lys 59	N(CE3/CZ3)	3.78
Lys 59	O(CA)	6.52
Arg 60	N(N)	5.11
Arg 60	O(N)	5.63
Lys 63	N(N)	3.61
Lys 63	O(N)	2.25
Lys 65	N(C)	1.32
Lys 65	O(C)	4.07
Pro 156	O(CE2)	6.63
His 157	N(NE1)	5.98
His 157	O(CZ2)	5.90
Pro 158	N(CZ2)	4.47
Pro 158	O(CZ2)	6.07
Glu 159	N(CZ2)	4.12
Glu 159	O(NE1)	3.31
	nonpolar groups and aromatic residues	
Tyr 39	CB, CG, CD1, CD2, **CE1**, CE2, CZ	3.88
His 155	CE1	6.40
His 157	CB, CG, CD2, **CE1**	3.52
Pro 158	CB, CG, **CD**	3.69
Val 58	**CB**, CG1, CG2	5.50
Lys 63	**CB**, CG, CD, CE	3.23
Lys 65	**CB**, CG, CD, CE	3.46

*R is the minimal distance between a residue involved in the microenvironment of tryptophan residue and its indole ring.

Table 5. Characteristics of the Trp 133 microenvironment in bOBPwt and GCC-bOBP.

bOBPwt			GCC-bOBP		
residue	atom	R*, Å	residue	atom	R*, Å
		polar groups			
Tyr 21B	OH(CZ2)	4.36	Tyr 21	OH(NE1)	5.03
Thr 136	OG1 (CA)	4.35	Thr 136	OG1 (CA)	4.44
Lys 143	NZ (CE3)	3.35	HOH 1087	(CH2)	4.99
HOH 218A	(CE3/CZ3)	4.69			
HOH 254A	(NE1)	3.94			
HOH 232B	(NE1)	3.27			
HOH 283B	(CZ2)	5.83			
		peptide bonds			
Leu 129	N(N)	6.23	Leu 129	O(N)	2.97
Leu 129	O(N)	3.10	Phe 132	O(N)	2.26
Glu 130	N(CD1)	4.75	Lys 134	N(C)	1.33
Glu 130	O(N)	3.33			
Phe 132	N(N)	2.85			
Phe 132	O(N)	2.26			
Lys 134	N(C)	1.33			
Lys 134	O(O)	3.28			
Thr 136	N(O)	3.37			
Thr 136	O(O)	5.01			
Lys 143	N(CZ3)	5.56			
Lys 143	O(CH2)	5.36			
Val 146	N(CH2)	6.50			
Val 146	O(CH2)	6.63			
		nonpolar groups and aromatic residues			
Tyr 21B	CB, CG, CD1, CD2, CE1, **CE2**, CZ	4.17	Tyr 21	CB, CG, CD1, CD2, CE1, **CE2**, CZ	3.96
Phe 132	CA, **C,** CB, CG, CD1, CD2, CE1, CE2, CZ	1.34	Phe 132	CA, **C,** CB, CG, CD1, CD2, CE1, CE2, CZ	1.33
Leu 129	CA, **C**, CB, CG, CD1, CD2	3.90	Leu 129	CA, **C**, CB, CD2	4.15
Lys 134	**CA**, C, CB, CG, CD	2.43	Val 146	CB, CG1, **CG2**	3.98
Val 146	CB, CG1, **CG2**	3.69	Lys 143	**CA**, CB, CG	4.55
Lys 143	CA, C, CB, **CG**, CD, CE	3.75			

*R is the minimal distance between a residue involved in the microenvironment of tryptophan residue and its indole ring.

Table 6. The evaluation of secondary structure of the recombinant bOBPwt and its mutant forms using Provencher's algorithm[2].

	α	β	turn	unordered
bOBPwt	0.133	0.359	0.204	0.297
bOBPwt/OCT	0.113	0.354	0.207	0.311

bOBP-Gly121+	0.085	0.400	0.208	0.303
bOBP-Gly121/OCT	0.112	0.407	0.200	0.272
GCC-bOBP	0.134	0.353	0.208	0.293
GCC-bOBP/OCT	0.145	0.344	0.217	0.288
GCC-bOBP W17F	0.077	0.415	0.209	0.299
GCC-bOBP W17F/OCT	0.087	0.429	0.206	0.276
GCC-bOBP W133F	0.154	0.356	0.206	0.269
GCC-bOBP W133F/OCT	0.172	0.352	0.200	0.275

1. Stepanenko OV, Stepanenko OV, Staiano M, Kuznetsova IM, Turoverov KK, et al. (2014) The quaternary structure of the recombinant bovine odorant-binding protein is modulated by chemical denaturants. PLoS One 9: e85169.
2. Provencher SW, Glockner J (1981) Estimation of globular protein secondary structure from circular dichroism. Biochemistry 20: 33-37.

1

3D structure of bOBP

Figure 1. 3D structure of bOBP . The individual subunits in the protein are in gray and orange. The tryptophan residues in the different subunits are indicated in red and blue. The Lys 121 residue after which an extra glycine residue are inserted in the mutant form bOBP-Gly121+ is drown in green. Additionally the residues Trp 64 and His 156 (yellow) are substituted for cysteine in the mutant form GCC-bOBP. The drawing was generated based on the 1OBP file (Tegoni et al. 1996) from PDB (Dutta et al. 2009) using the graphic software VMD (Hsin et al. 2008) and Raster3D (Merritt & Bacon 1977) .

PeerJ PrePrints | https://dx.doi.org/10.7287/peerj.preprints.1445v1 | CC-BY 4.0 Open Access | rec: 23 Oct 2015, publ: 23 Oct 2015

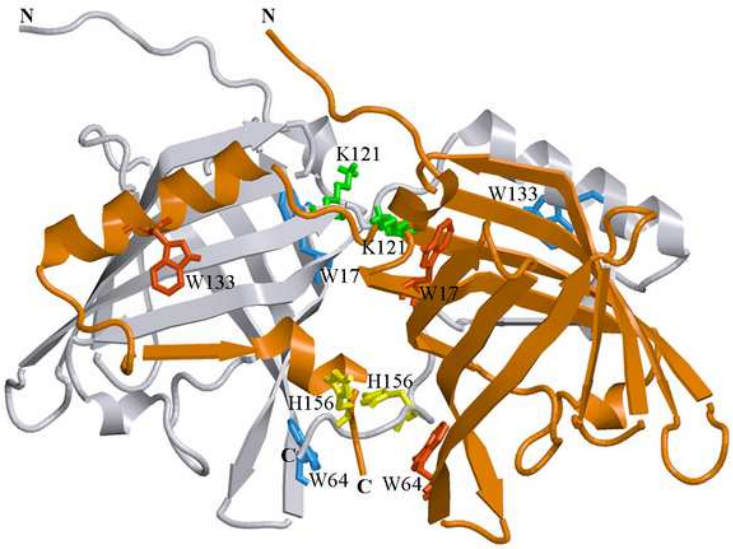

Table 2(on next page)

Sequence peculiarities of various bPDB forms.

Figure 2. Sequence peculiarities of various bPDB forms. The comparison of the primary sequence for the recombinant bOBPwt and its mutant forms bOBP-Gly121+ and GCC- bOBP, which are not able to form domain-swapped dimers. The mutant forms GCC-bOBP-W17F and GCC-bOBP-W133F designed to contain a single tryptophan residue were produced to investigate the peculiarities of the microenvironment of the tryptophan residues.

PeerJ PrePrints | https://dx.doi.org/10.7287/peerj.preprints.1445v1 | CC-BY 4.0 Open Access | rec: 23 Oct 2015, publ: 23 Oct 2015

1. bOBPwt – wild type protein forms dimer via the domain-swapping mechanism. The protein has 3 tryptophan residues.

AQEEEAEQNL SELSGP**W**RTV YIGSTNPEKI QENGPFRTYF RELVFDDEKG TVDFYFSVKR
DGK**W**KNVHVK ATKQDDGTYV ADYEGQNVFK IVSLSRTHLV AHNINVDKHG QTTELTGLFV
KLNVEDEDLE KF**W**KLTEDKG IDKKNVVNFL ENEDHPHPE

2. bOBP-Gly121+ – the introduction of an extra glycine residue after the bOBP residue 121 is proposed to inhibit dimer formation as a result of the increased mobility of the loop connecting α-helix and 8th β-strand of the β-barrel. The protein contains 3 tryptophan residues as well.

AQEEEAEQNL SELSGP**W**RTV YIGSTNPEKI QENGPFRTYF RELVFDDEKG TVDFYFSVKR
DGK**W**KNVHVK ATKQDDGTYV ADYEGQNVFK IVSLSRTHLV AHNINVDKHG QTTELTGLFV
K**G**LNVEDEDLE KF**W**KLTEDKG IDKKNVVNFL ENEDHPHPE

3. GCC- bOBP (bOBP-Gly121+-W64C-H155C) – the substitutions W64C and H155C result in the restoration of the disulfide bond which is necessary for the additional stabilization of the protein. The protein has only 2 tryptophan residues.

AQEEEAEQNL SELSGP**W**RTV YIGSTNPEKI QENGPFRTYF RELVFDDEKG TVDFYFSVKR
DGK**C**KNVHVK ATKQDDGTYV ADYEGQNVFK IVSLSRTHLV AHNINVDKHG QTTELTGLFV
K**G**LNVEDEDLE KF**W**KLTEDKG IDKKNVVNFL ENED**C**PHPE

4. GCC-bOBP-W17F (bOBP-Gly121+-W64C-H155C-W17F) – the protein contains a single tryptophan residue which allows the investigation of the features of the microenvironment of this residue.

AQEEEAEQNL SELSGP**F**RTV YIGSTNPEKI QENGPFRTYF RELVFDDEKG TVDFYFSVKR
DGK**C**KNVHVK ATKQDDGTYV ADYEGQNVFK IVSLSRTHLV AHNINVDKHG QTTELTGLFV
K**G**LNVEDEDLE KF**W**KLTEDKG IDKKNVVNFL ENED**C**PHPE

5 GCC-bOBP-W133F (bOBP/Gly121+/W64C/H155C/W133F) – the protein has a single tryptophan residue as well.

AQEEEAEQNL SELSGP**W**RTV YIGSTNPEKI QENGPFRTYF RELVFDDEKG TVDFYFSVKR
DGK**C**KNVHVK ATKQDDGTYV ADYEGQNVFK IVSLSRTHLV AHNINVDKHG QTTELTGLFV
K**G**LNVEDEDLE KF**F**KLTEDKG IDKKNVVNFL ENED**C**PHPE

2

Intrinsic disorder propensity of the wild type bOBP and its mutants .

Figure 3. Intrinsic disorder propensity of the wild type bOBP and its mutants . **A** . Per-residue disorder propensity of the wild type bOBP evaluated by members of the PONDR family, PONDR® VLXT (Stepanenko et al. 2015) (green line), PONDR® VSL2 (Stepanenko et al. 2014a) (blue line), PONDR® FIT (Xue et al. 2010) (red line) and PONDR® VL3 (pink line). Localization of known elements of the bOBP secondary structure is shown by colored bars at the bottom of the plot. Light pink shadow around the PONDR® FIT curve represents distribution of errors in the disorder score evaluation. **B** . Effects of mutations on the intrinsic disorder propensity of bOBP evaluated by PONDR® VSL2.

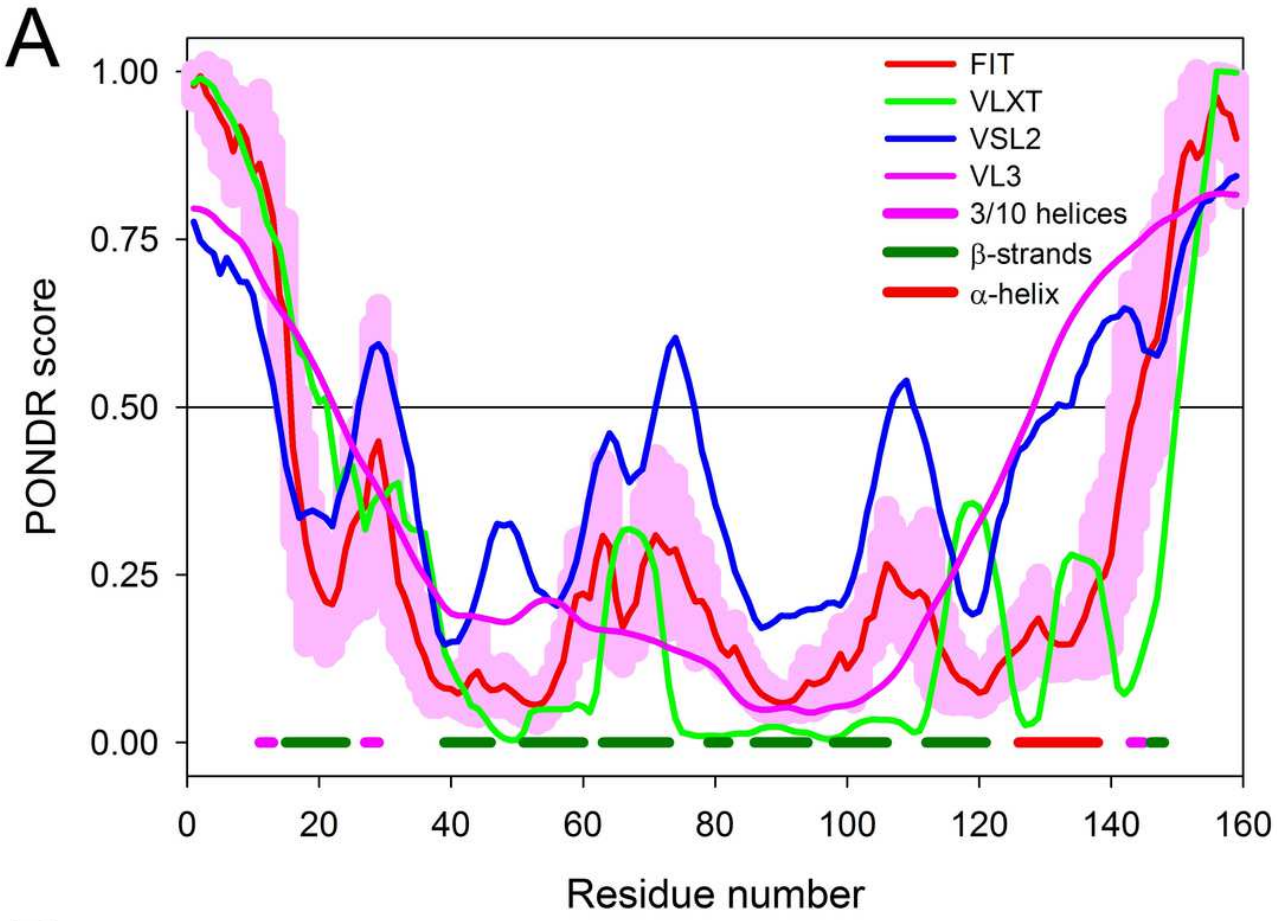

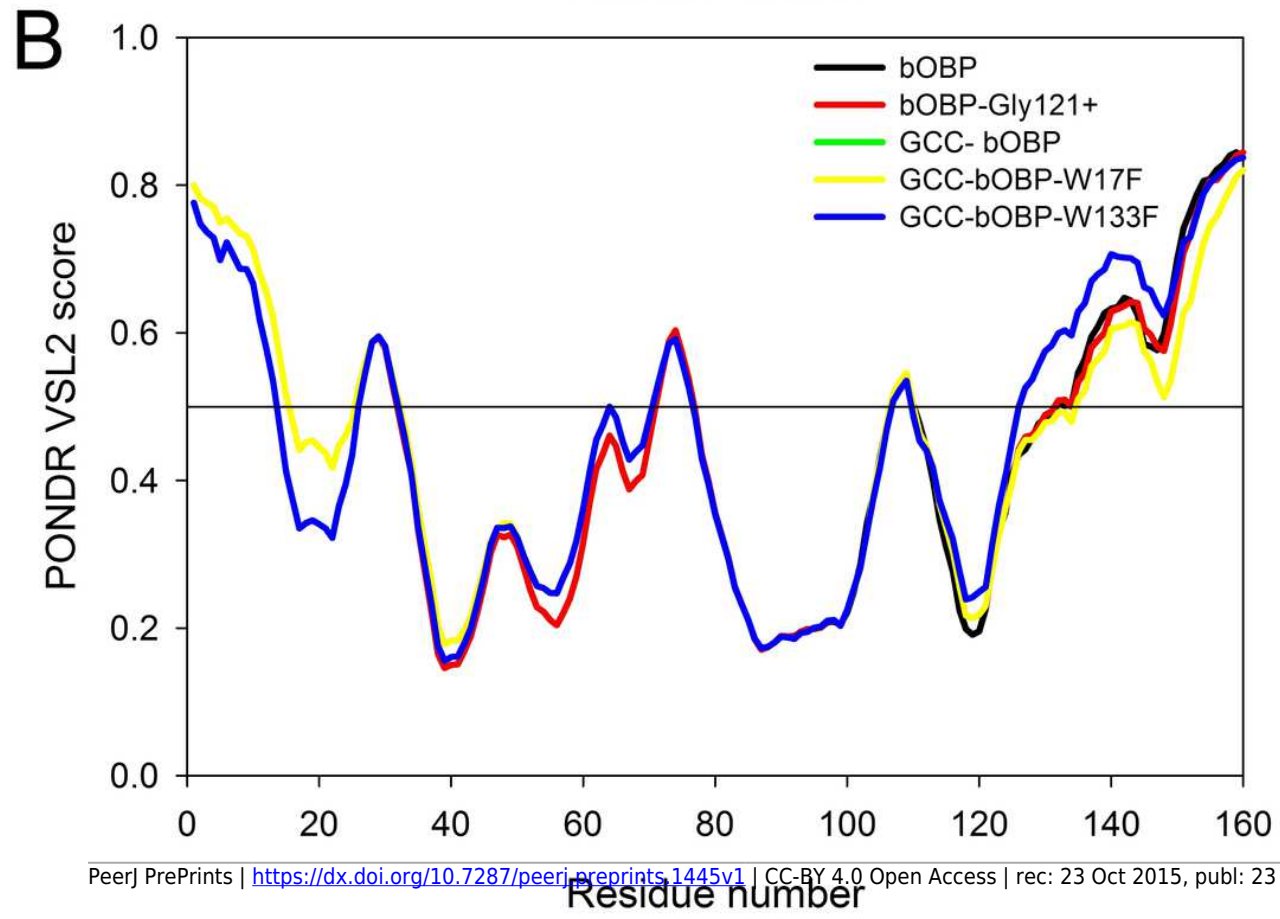

PeerJ PrePrints | https://dx.doi.org/10.7287/peerj.preprints.1445v1 | CC-BY 4.0 Open Access | rec: 23 Oct 2015, publ: 23 Oct 2015

3

GdnHCl-induced conformational changes in bOBP (data for this figure aretaken from (Stepanenko et al. 2014b)).

Figure 4. GdnHCl-induced conformational changes in bOBP (data for this figure are taken from (Stepanenko et al. 2014b)). **A** . changes in fluorescence intensity at 320 nm, λ_{ex} =297 nm; **B** . changes in parameter *A*, λ_{ex} =297 nm; **C** . changes in fluorescence anisotropy at the emission wavelength 365 nm, λ_{ex} =297 nm; **D** . changes in the ellipticity at 222 nm. The measurements were preceded by incubating the protein in a solution with the appropriate GdnHCl concentration at 4ºC for 24 h. The open symbols indicate unfolding, whereas the closed symbols represent refolding. Changes in bOBP hydrodynamic dimensions for the different structural states were followed by the changes in the elution profiles for bOBP after pre-incubation for 24 h (solid lines) and 43 h (dashed line) with GdnHCl at the concentrations 0.0 (**E**), 0.5 (**F**) and 1.5 (**G**) for the denaturation process.

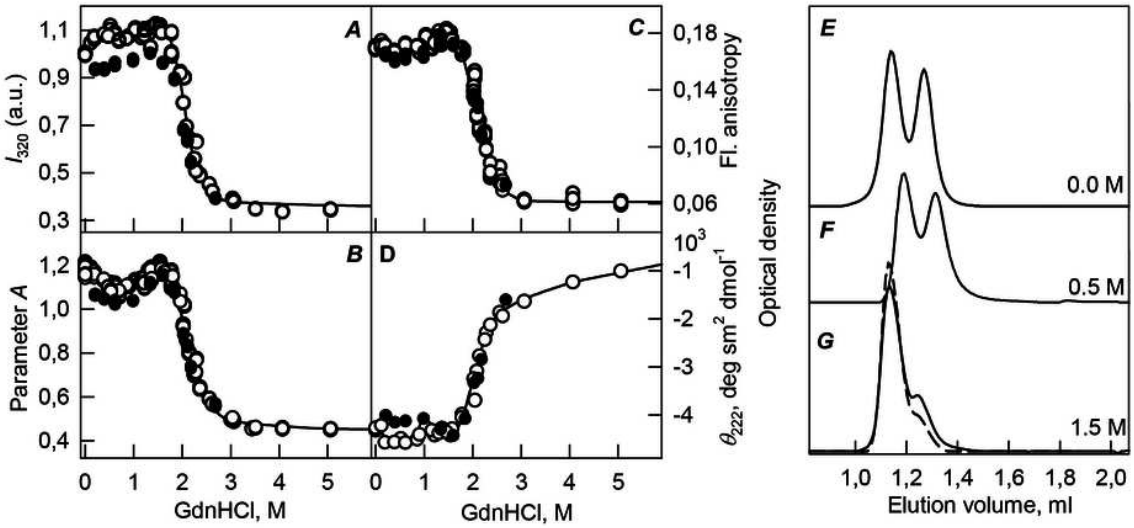

Table 3(on next page)

Hydrodynamic characteristics of the bOBP and its mutants.

Figure 5. **Hydrodynamic characteristics of the bOBP and its mutants.** The changes of hydrodynamic dimensions of recombinant bOBP (1) and its mutant forms bOBP-Gly121+ (2), GCC-bOBP (3), GCC-bOBP-W17F (4) and GCC-bOBP-W133F (5) in the absence (solid lines) and the presence of OCT (dotted lines).

PeerJ PrePrints | https://dx.doi.org/10.7287/peerj.preprints.1445v1 | CC-BY 4.0 Open Access | rec: 23 Oct 2015, publ: 23 Oct 2015

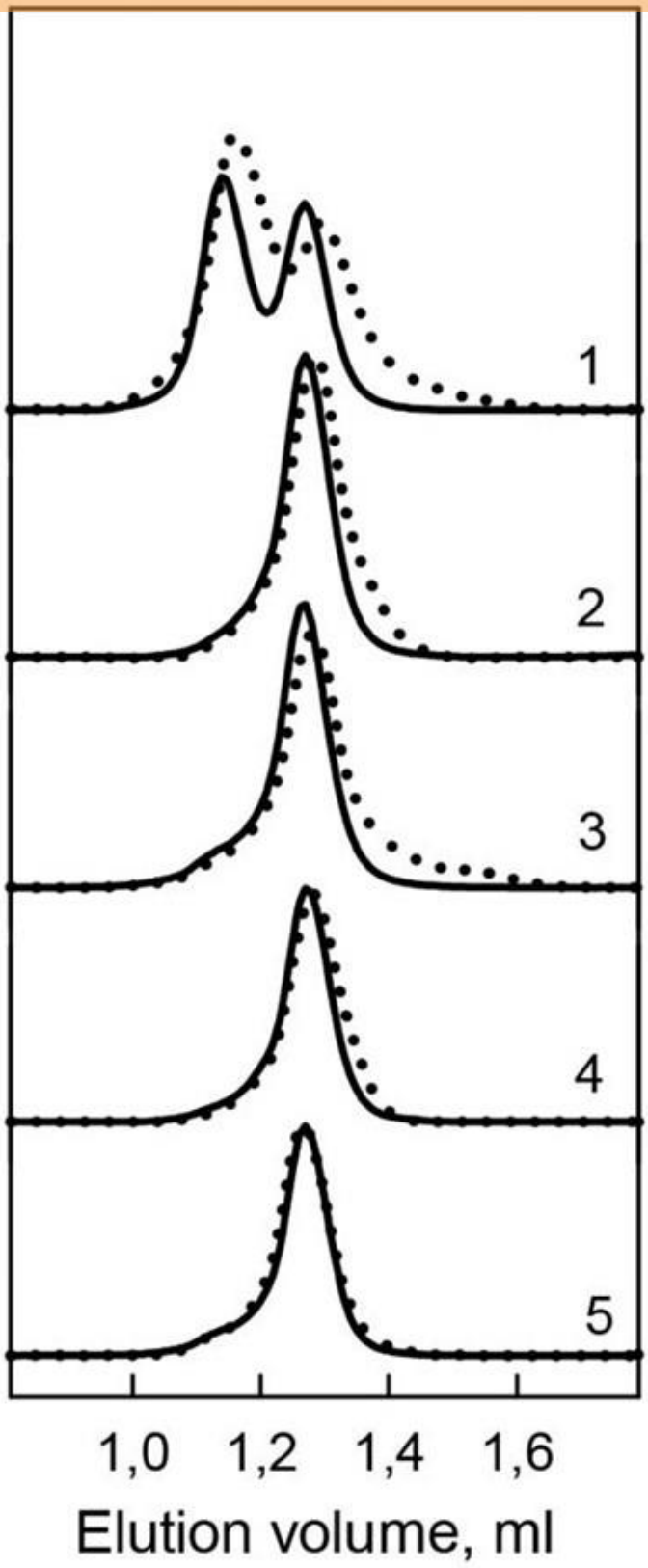

4

Tertiary structure changes for bOBP (red) and its mutant formsbOBP-Gly121+ (green), GCC-bOBP (blue), GCC-bOBP-W17F (gray) and GCC-bOBP-W133F(dark yellow) in different structural states

Figure 6. Tertiary structure changes for bOBP (red) and its mutant forms bOBP-Gly121+ (green), GCC-bOBP (blue), GCC-bOBP-W17F (gray) and GCC-bOBP-W133F (dark yellow) in different structural states are indicated by intrinsic tryptophan fluorescence (λ_{ex}=297 nm). The spectra shown are for the protein in buffered solution (solid line), in the presence of natural ligand OCT (dotted line) and in the presence of 3.5 M GdnHCl (dashed line). The corresponding spectra in light blue were obtained as a sum of the spectra for GCC-bOBP-W17F and GCC-bOBP-W133F.

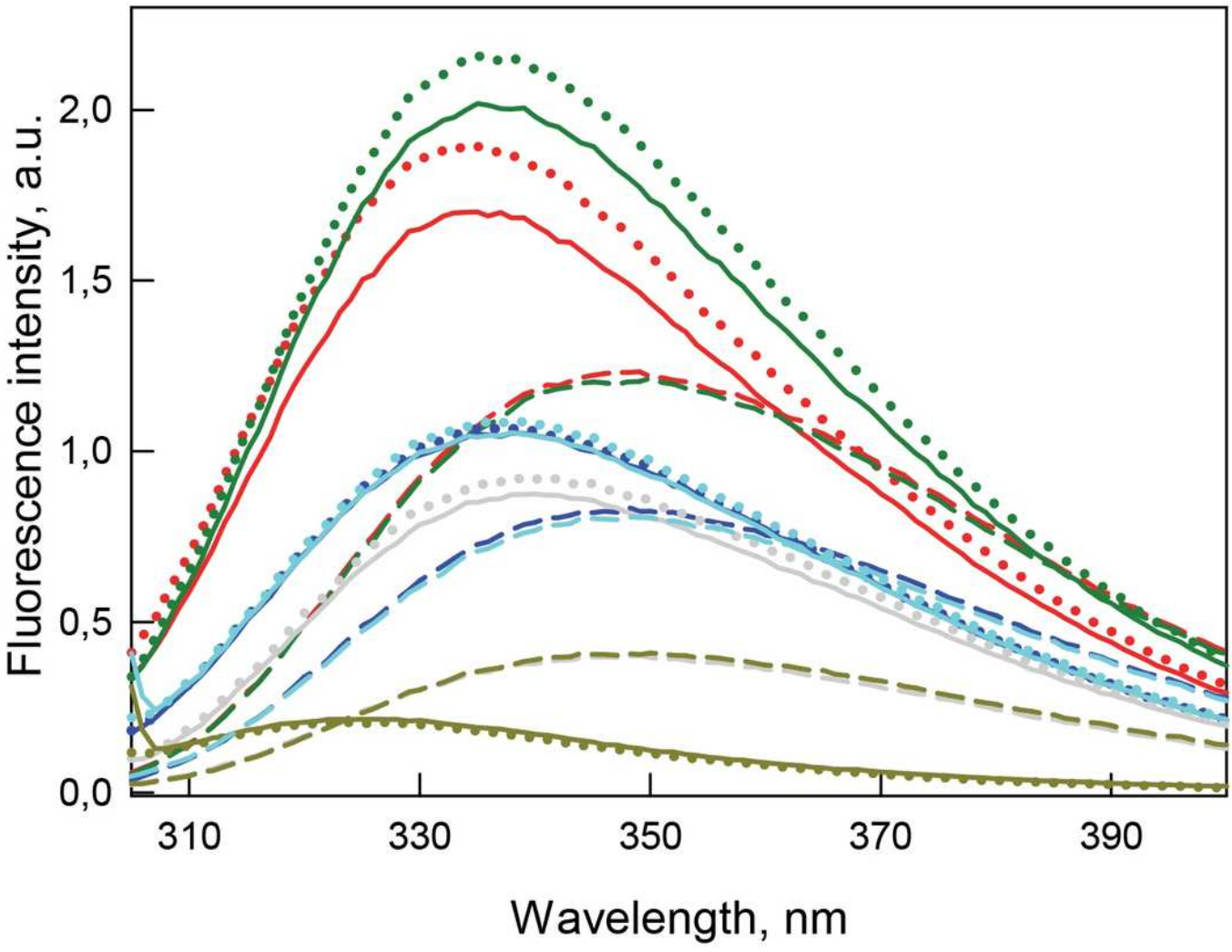

5

Tertiary structure for bOBP (red) and its mutant forms bOBP-Gly121+(green), GCC-bOBP (blue), GCC-bOBP-W17F (gray) and GCC-bOBP-W133F (dark yellow)

Figure 7. Tertiary structure for bOBP (red) and its mutant forms bOBP-Gly121+ (green), GCC-bOBP (blue), GCC-bOBP-W17F (gray) and GCC-bOBP-W133F (dark yellow) in buffered solution are indicated by near-UV CD spectra. The spectrum in light blue was obtained as a sum of the spectra for GCC-bOBP-W17F and GCC-bOBP-W133F.

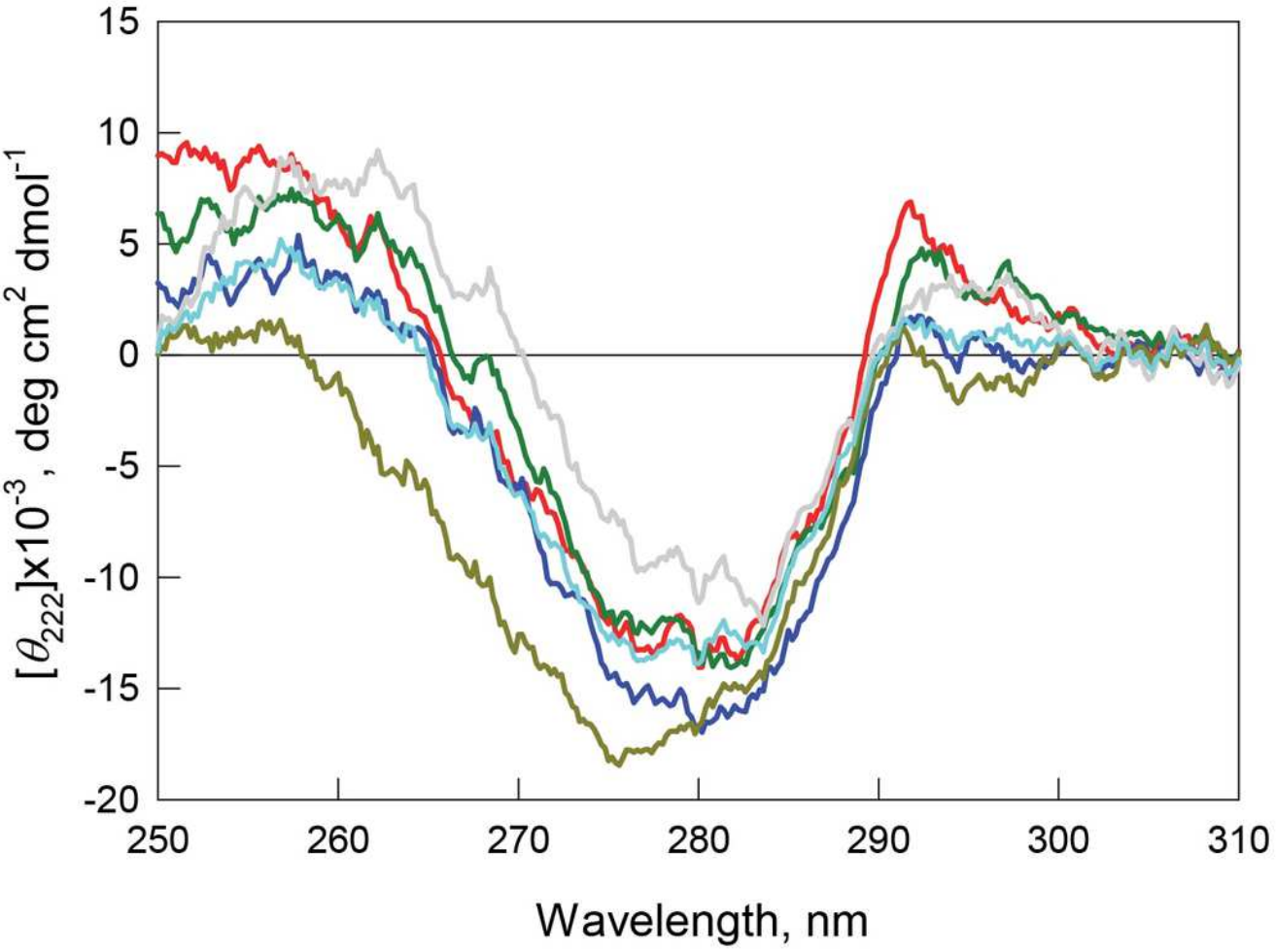

The microenvironment of Trp 17 (*A*)and Trp 64 (*B*) in bOBP.

Figure 8. The microenvironment of Trp 17 (*A*) and Trp 64 (*B*) in bOBP. The spatial orientation of lysine residues relative the indole ring of tryptophan residues is shown. The drawing was generated based on the 1OBP file (Tegoni et al. 1996) from PDB (Dutta et al. 2009) using the graphic software VMD (Hsin et al. 2008) and Raster3D (Merritt & Bacon 1977) .

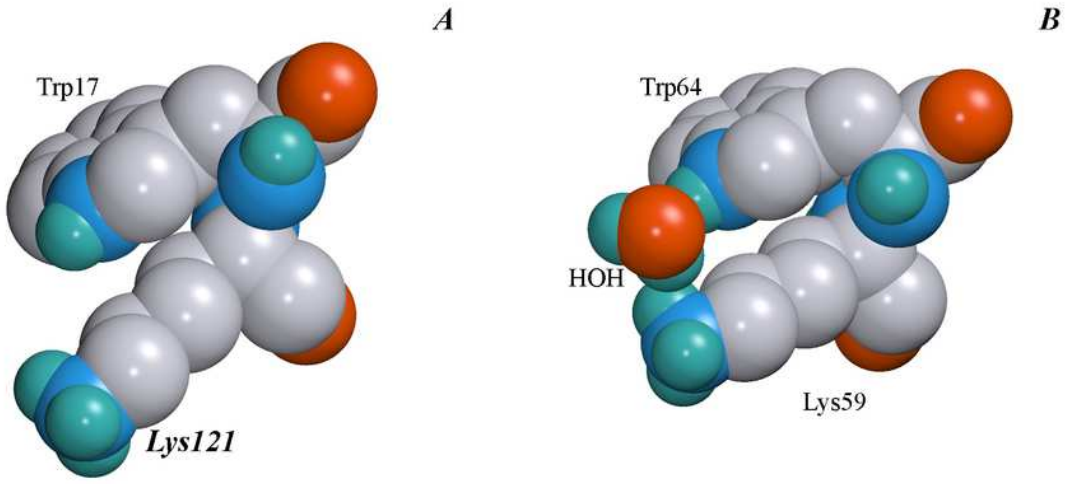

Secondary structure for bOBP (red) and itsmutant forms bOBP-Gly121+ (green), GCC-bOBP (blue), GCC-bOBP-W17F (gray) andGCC-bOBP-W133F (dark yellow)

Figure 9. Secondary structure for bOBP (red) and its mutant forms bOBP-Gly121+ (green), GCC-bOBP (blue), GCC-bOBP-W17F (gray) and GCC-bOBP-W133F (dark yellow) in buffered solution are indicated by far-UV CD spectra.